Electronic Supplementary Material (ESI) for Molecular Systems Design & Engineering.

Supporting information

Heteroatom Engineering of Polymeric Carbon Nitride Heterojunctions for Boosting Photocatalytic Reduction of Hexavalent Uranium

Fengtao Yu,[a§] Zhiwu Yu,[b§] Zhenzhen Xu,[a] Jianbo Xiong,[a] Qiangwen Fan,[a] Xuefeng Feng,[a] Yuan Tao,[a] Jianli Hua[c] and Feng Luo[a]*

[a] *State Key Laboratory of Nuclear Resources and Environment, School of Chemistry, Biology and Materials Science, East China University of Technology, Nanchang, 330013, P. R. China.*

[b]*High Magnetic Field Laboratory, Chinese Academy of Sciences, Hefei 230031, Anhui, China.*

[c]*Key Laboratory for Advanced Materials, Institute of Fine Chemicals, East China University of Science and Technology, 200237, Shanghai, China.*

Table of Contents

S1 Materials

S2 Synthesis

S3 Characterization

S4 Electrochemical analysis

S5 Photocatalytic reduction and removal of UO_2^{2+} experiments

S6 DFT Calculation Methods

S7 Corresponding figure in the article

S8 Corresponding table in article

S9 References

S1 Materials

2,7-dibromo-9H-carbazole, 2,7-dibromo-9,9-dioctyl-9H-fluorene (**1a**), 4,7-bis(4,4,5,5-tetramethyl-1,3,2-dioxaborolan-2-yl)benzo[c][1,2,5]thiadiazole, anhydrous potassium carbonate，tetrakis(triphenylphosphine)-palladium(0) [$Pd(PPh_3)_4$], Toluene，Aliquat 336 and arsenazo-III were purchased from Sigma-Aldrich, respectively. $UO_2(NO_3)_2 \cdot 6H_2O$ was obtained from Hubei Chushengwei Chemical Reagent Co., Ltd. and used as received unless indicated otherwise. 2,7-dibromo-9-(2-ethylhexyl)-9H-carbazole (**1b**) was synthesized according to previous paper [1]. Glassware was dried in oven prior to use. All chemical reactions were carried out under an inert nitrogen atmosphere.

S2 Synthesis

S2.1 Synthesis of 2,7-dibromo-9-(2-ethylhexyl)-9H-carbazole (1b)

Under nitrogen atmosphere，3-(bromomethyl)heptane (1160 mg, 6 mmol), 2,7-dibromo-9H-carbazole (1115.8 mg, 4 mmol) and sodium hydride (144 mg, 6 mmol) were dissolved in 100 mL ultra-dry tetrahydrofuran (THF) solution. The mixture was stirred at 70 °C for 24 h. After being cooled down, the mixture was poured into water and the crude product was extracted with CH_2Cl_2, the organic phase was concentrated under reduced pressure and purified by column chromatography on silica gel with petroleum ether (PE) as the eluent to yield the oily liquid product **1b** (1300 mg, 91%). ^1H NMR ($CDCl_3$, 400 MHz), δ (TMS, ppm): 8.11 (m, 2H), 7.54–7.51 (m, 2H), 7.22 (d, J = 8.0 Hz, 2H), 4.08–4.06 (m, 2H), 2.01–1.94 (m, 1H), 1.35–1.24 (m, 8H), 0.90–0.86 (m, 3H), 0.85–0.83 (m, 3H). ^{13}C NMR ($CDCl_3$, 100 MHz), δ (TMS, ppm): 139.67, 128.93, 123.33, 123.13, 111.91, 110.62, 47.55, 39.32, 30.96, 29.78, 28.77, 24.36, 23.05, 14.07, 10.91. HRMS (ESI-MS) m/z calcd. For $C_{20}H_{23}Br_2N$: 435.0197. [$M + H^+$]. Found: 436.0278.

S2.2 Synthetic target organic polymerization PFB and PCB

The target D-A conjugated polymers **PFB** and **PCB** were synthesized by the Pd(0)-catalyzed Suzuki–Miyaura polymerization reactions.

PFB: To a mixture of **1a** (546.15 mg, 1.0 mmol), 4,7-bis(4,4,5,5-tetramethyl-1,3,2-dioxaborolan-2-yl)benzo[c][1,2,5]thiadiazole (388 mg, 1.0 mmol), and

Tetrakis(triphenylphosphine)palladium (23.0 mg, 0.02 mmol) were added two drops of Aliquat 336, degassed toluene (10 mL), 2 M aqueous solution of potassium carbonate (3.0 mL, 6 mmol). Then the mixture was heated to 90℃ with vigorous stirring under nitrogen for 48 h. After being cooled down, the mixture was poured into 300 mL methanol. The precipitate was collected by filtration and then extracted with DCM. The organic phase was concentrated to an appropriate volume. The crude product was obtained by pouring the concentrated solution into methanol (200 mL). After Soxhlet extraction with acetone for 24 h, the polymer was further purified with reprecipitation in DCM/methanol several times to give **PFB** as a light-yellow fiber (818 mg, Yield is 86%). GPC: number-average molecular weight $M_n = 5.03 \times 10^4$, PDI = 1.78 (PDI: polydispersity index, polystyrene as standard). ^1H NMR ($CDCl_3$, 400 MHz), δ (TMS, ppm): 8.12-8.10 (m, 2H), 8.03 (s, 2H), 7.99-7.95 (m, 4H), 2.12-2.15 (m, 4H), 1.19-1.16 (m, 22 H), 0.82-0.79 (m, 8 H). ^{13}C NMR ($CDCl_3$, 100 MHz), δ (TMS, ppm): 154.1, 151.81, 140.93, 136.51, 133.65, 128.36, 128.02, 124.07, 120.09, 55.47, 40.26, 31.87, 30.15, 29.31, 29.28, 24.09, 22.64, 14.10.

PCB: The same synthesis method gets orange powder **PCB** (655 mg, Yield is 79.7%), only the comonomer has **1b** (434 mg, 1 mmol) instead of **1a**. GPC: $M_n = 3.67 \times 10^4$, PDI = 2.56. ^1H NMR ($CDCl_3$, 400 MHz), δ (TMS, ppm): 8.84-8.58 (m, 2H), 8.21-7.93 (m, 2H), 7.69-7.52 (m, 2H), 7.45-7.33 (m, 2H), 4.29-3.93 (m, 2 H), 2.20-1.99 (m, 1 H), 1.34-1.26 (m, 8 H), 0.90-0.85 (m, 6 H). ^{13}C NMR ($CDCl_3$, 100 MHz), δ (TMS, ppm): 154.48, 127.68, 123.23, 31.07, 28.93, 24.43, 23.14, 14.13, 10.95.

S2.3 Synthetic of g-C_3N_4 (Mark as CN)

Graphitic carbon nitride was prepared according to published procedures with some modifications. [1] Typically, 20 g of urea was put in a ceramic container with a cover and heated under static air at 550 °C for 2 h with a ramping rate of 5 °C min^{-1}. The resultant yellow powder was collected for use without further treatment and denoted as CN.

S2.4 Synthesis of the PFB/CN and PCB/CN heterojunctions photocatalysts

A certain amount of polymer **PFB** (**PCB**) was dissolved in chloroform, and then 100 mg of CN was added to the above solution. The mixture was vigorous stirring in the dark for 12 h. The $CHCl_3$ suspensions containing polymers/CN heterojunction were then evaporated at 50 °C to obtain the powdered X-**PFB**/CN and X-**PCB**/CN, in which X indicates the quality of the added polymer (X = 1, 3, 5, 7, 9, and 10).

S3 Characterization

^1H and ^{13}C NMR spectra were obtained in deuterated solvents on Bruker AM 400 MHz using tetramethylsilane (TMS) as an internal standard. High-resolution mass spectra (HRMS) measurements were performed using a Waters LCT Premier XE spectrometer. UV-vis diffuse reflection spectrum was obtained by UV-vis spectrophotometer (UV-2550, Shimadzu, Japan). The photoluminescence (PL) spectra were acquired on an Edinburgh FI/FSTCSPC 920 spectrophotometer. The FTIR spectra were recorded on NICOLET 380 spectrometer using a standard KBr pellet technique in the frequency range of 4000-400 cm^{-1}. Crystal structure was characterized using X-ray diffraction (XRD, Rigaku RINT-2000 instrument equipped with Cu Kα. The surface chemical component and oxidation states of photocatalysts were investigated with X-ray photoelectron spectroscopy (XPS) measurements were taken by using a Thermo Scientific ESCALAB 250 Xi spectrometer equipped with an Al anode (Kα = 1486.7 eV). The binding energies of XPS spectrum were referenced C 1s at 284.6 eV. SEM and EDS measurements were carried out using a Hitachi S-4800 microscope.

S4 Electrochemical analysis

The Mott-Schottky curves (M-S), transient photocurrent responses (I–t) and electrochemical impedance spectra (EIS) of composite photocatalyst samples were investigated on a CHI650E electrochemical workstation with a three-electrode (Pt wire, Pt plate, and Ag/AgCl as working, counter, and reference electrode, respectively) system. An aqueous solution of 0.5 m Na_2SO_4 was used as the supporting electrolyte and a 300 W Xe-lamp with a cutoff filter ($\lambda \geq 400$ nm) served as the light source. The films electrodes were prepared as follows: 25 mg of the as-synthesized photocatalysts (CN, **PFB**/CN and **PCB**/CN) was separately ground with 10 μL of a Nafion (5%) aqueous solution and 50 μL of ethanol to make slurry. The slurry was then coated onto

ITO glass electrodes with an active area of 0.25 cm^2, and these electrolytes were dried at 120 °C for 1 h to evaporate the solvent in muffle furnace. The photocurrent intensity of as-prepared electrodes was measured at 0 V versus Ag/AgCl with the light on and off. EIS was determined over the frequency range of 10^2–10^6 Hz with an ac amplitude of 10 mV at the open circuit voltage under room-light illumination. The Mott-Schottky plots were recorded by using three different frequencies of the AC potential at 1000, 1500 and 2000 Hz. The donor carrier concentration was calculated from Eq. (1)

$$\frac{1}{C^2_{SC}} = \frac{2}{\varepsilon_0 \varepsilon_r e A^2 N_d}(\Psi_{SC} - \frac{kT}{e}) \times 100\% \tag{1}$$

where e is the elemental charge: 1.6 × 10^{-19} C, A is the active area of work electrode, ε_0 is the permittivity of vacuum: 8.85 × 10^{-14} F/cm, ε is the relative permittivity of the material, the value is 5.5 for g-C_3N_4. k is the bolztaman constant, and T is the temperature.

S5 Photocatalytic reduction and removal of UO_2^{2+} experiments

All photocatalytic experiments were conducted in a jacketed quartz beaker photoreactor cooled by circulating water. Typically, 50 mg photocatalyst was placed into 100 mL of aqueous solutions containing 100 ppm U(VI) at pH 4.0 and under stirring continuously. The values of pH in suspension were adjusted using NaOH (0.1 M) or H_2SO_4 (0.1 M) solution. Before irradiation, the reaction system was bubbled with N_2 (or O_2) in dark for 60 min to maintain anaerobic conditions and reach the adsorption-desorption equilibrium. Then, the suspension was illuminated using a 300 W Xe lamp (Light source model: SHX-F300, $\lambda \geq 400$ nm). At given times, aliquot (2 mL) of the solution were pipetted and filtered through 0.45 μm Nylon syringe filters. The UO_2^{2+} content in the supernatant solution was detected with UVmini-1240 by Arsenazo-III Spectrophotometric technology at 652 nm.[2] This measured absorbance with illumination time was converted to photoreduction efficiency of UO_2^{2+} in accordance with the equation (1):

$$RE = \frac{(C_0 - C_t)}{C_0} \times 100\% \tag{2}$$

Where, RE is the uranium reduction efficiency; C_0 and C_t are the concentration (mg/L) of uranium at initial and contact time t (min), respectively.

Removal of UO_2^{2+}: Reducing the soluble and environmentally mobile U^{VI} to the less soluble and relatively immobile U^{IV} species for uranium immobilization is considered as a promising strategy for achieving the removal of uranium.

Recycling of photocatalyst: After photoreduction reaction, photocatalyst was collected by centrifugation, and washed by the 1 M HNO_3 to eliminate UO_2 on the surface, and further washed with the deionized H_2O. Then, photocatalyst was dehydrated in vacuum at 60 ℃ for 8 h.

S6 DFT Calculation Methods

Density functional theory (DFT) calculations were performed using the Gaussian 09 program package. All structures and the frontier molecular orbitals were optimized without symmetry constrains at the B3LYP/6-31G* level. [3]

S7 Corresponding figure in the article

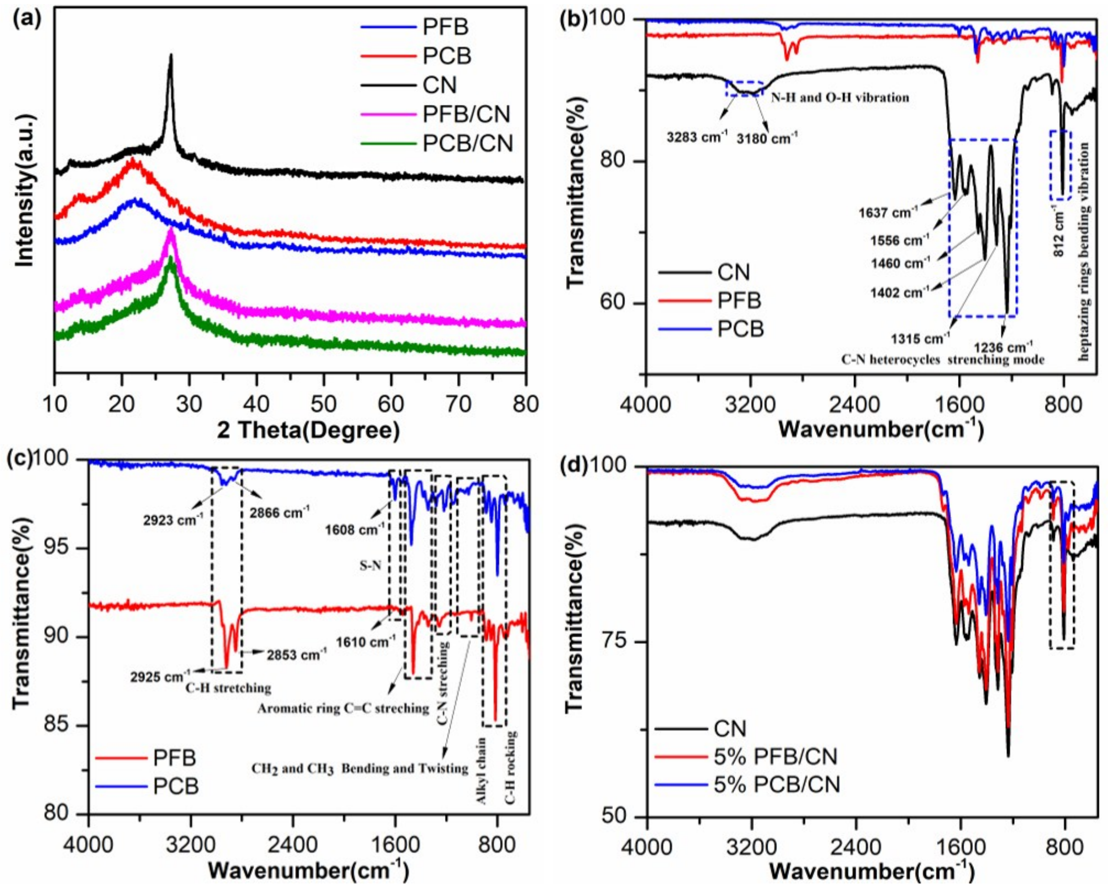

Fig. S1 (a) XRD diffraction patterns of **PFB**, **PCB**, CN, **PFB**/CN and **PC**B/CN; (b) FTIR spectra of CN, **PFB** and **PCB**; (c) FTIR spectra of the **PFB** and **PCB** to show the detailed molecular structures; (d) FTIR spectra of **PFB**/CN and **PCB**/CN heterostructures.

The chemical structures of all the as-prepared samples were further confirmed by Fourier transform infrared (FTIR) spectra. In Fig. S1b, the raw CN exhibits typical characteristic peaks: the sharp peak at 812 cm^{-1} is the characteristic breathing mode of s-triazine ring system, a series of peaks located between 1236 to 1637 cm^{-1} are attributed to the typical stretching modes of C−N heterocycles in CN, while multiple broad peaks in 3000– 3500 cm^{-1} region belongs to N−H and O-H vibration. As for **PFB** and **PCB**, they possess strong transmittance because of the high rigidity. In order to clearly interpret the molecular structure of the polymer, the amplified infrared spectrum is shown in Fig. S1c. The characteristic peaks at 1610 cm^{-1} and 1608 cm^{-1} in **PFB** and **PCB** belongs to the stretching vibration of S–N. Both polymers show C–H stretching vibrations of the alkyl chain at 2800 – 3000 cm^{-1}, the skeleton mode of C= C group at 1340 cm^{-1} and 1520 cm^{-1}, and the stretching mode of C–N at around 1258 cm^{-1}, which excellently confirms the conjugated polymer structure. For polymer/CN heterostructures, the stretching of the C–N heterocycles and the bending vibration of the heptazine rings in CN became weaker with the increasing mass ratio of the polymer (Fig. S1d, FigS2a and FigS2b), indicating the formation of intermolecular interactions between CN and the rigid conjugated polymers within the polymers/CN heterostructures.

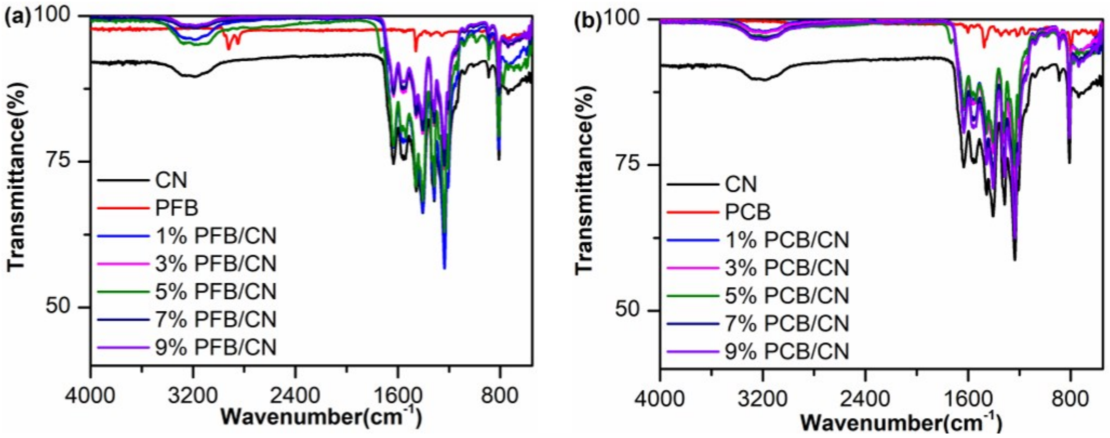

Fig.S2. FTIR spectra of (a) X-**PFB**/CN and (b) X-**PCB**/CN.

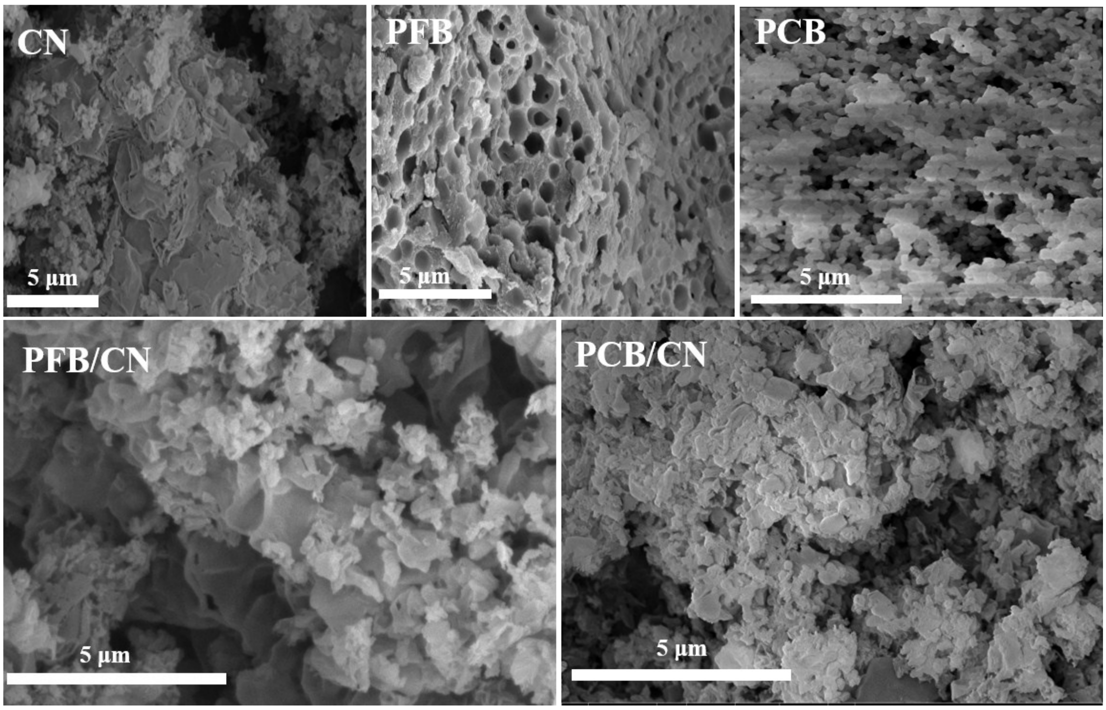

Fig.S3 Typical SEM images for CN, **PFB**, **PCB**, **PFB**/CN and **PCB**/CN.

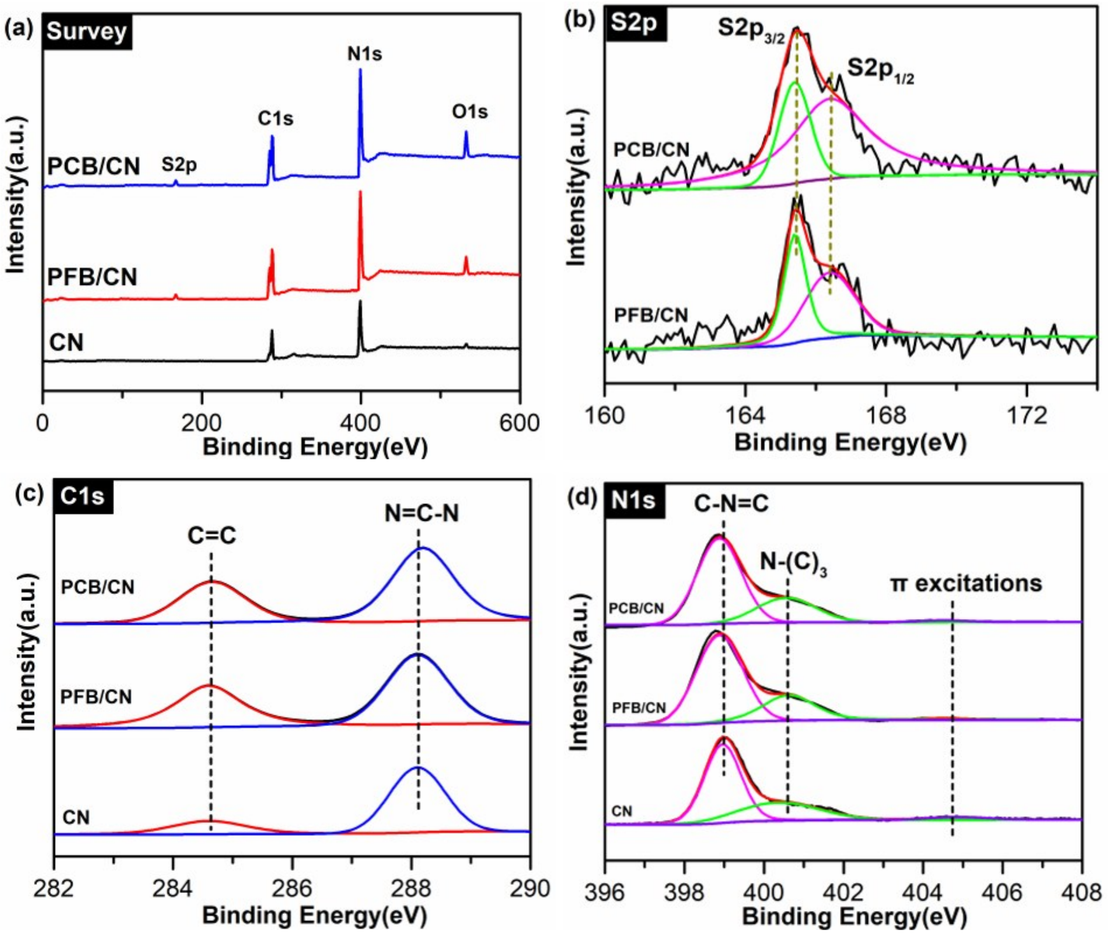

Fig.S4 High-resolution XPS spectra of CN, **PFB**/CN and **PCB**/CN composite heterojunctions: (a) Survey; (b) S2p; (c) C1s; (d) N1s.

X-ray photoelectron spectroscopy (XPS) was also undertaken to investigate the surface chemical compositions of the as-obtained samples. Seen from Fig.S4a and Table S1, all elements including C, N, O and S were detected in the survey spectra of **PFB**/CN and **PCB**/CN, which S element is derived from the polymer skeleton, demonstrating the coexistence of the two components of polymers and CN. It should be noted that O was found in all samples due to the adsorbed hydroxyl groups. Fig.S4b presents the corresponding deconvoluted S2p spectrum of **PFB**/CN and **PCB**/CN, two peaks at about 166.4 eV and 165.4 eV can be assigned to S2P3/2 and S2p1/2, respectively. In addition, Fig.S4c display the deconvoluted C1s spectrum of CN, **PFB**/CN and **PCB**/CN, The C 1s spectra could be deconvolved into two peaks at 284.60 eV and 288.10 eV for CN, 284.60 eV and 288.18 eV for **PFB**/CN, 284.60 eV and 288.1 eV for **PCB**/CN, which can be assigned to C=C and C-$(N)_3$, respectively. It is worth noting that **PFB**/CN and **PCB**/CN have the relatively higher peak area ratio of C=C (TableS3), suggesting the presence of aromatic rings derived from the polymer skeleton. In the deconvoluted N 1s spectrum of CN, three peaks at about 398.98 eV, 400.68 eV and 404.7 eV can be assigned to nitrogen in C= N–C, N–C_3 and π excitation, respectively. As shown in Fig.S4d, these three peaks can also be noticed in the **PFB**/CN (**PCB**/CN) composite, however, the corresponding peaks are shifted to lower binding energy compared to CN (TableS4), which may be due to the electronic transfer from polymer to CN via intermolecular π-π interaction. Furthermore, compared to CN, the peak area ratio of C=N–C for **PFB**/CN and **PCB**/CN increase from 65.5% to 71.8% and 71.0 %. Because the benzothiadiazole unit in the polymer backbone contains C=N–S, which increases the content of sp^2-hybridied N.

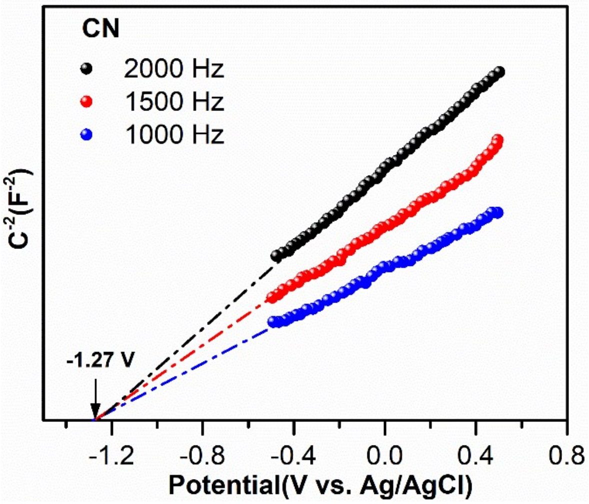

Fig.S5. The Mott-Schottky plots of CN.

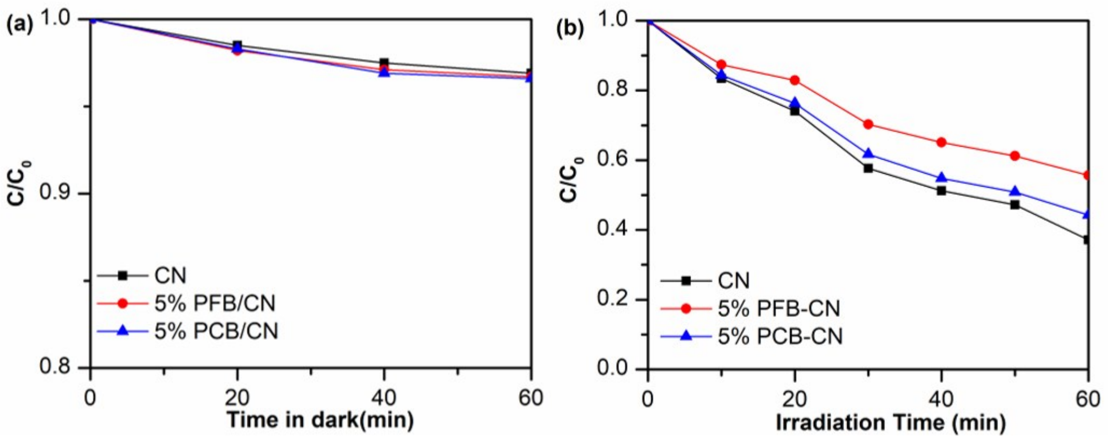

Fig.S6. (a) The variation of UO_2^{2+} concentration vs. dark time of CN, **PFB**/CN and **PCB**/CN; (b) The variation of UO_2^{2+} concentration vs. illumination time of CN, 5% **PFB**-CN and 5% **PCB**-CN.

(the **PFB**-CN and **PCB-CN** were obtained by physically mixing the two semiconductors)

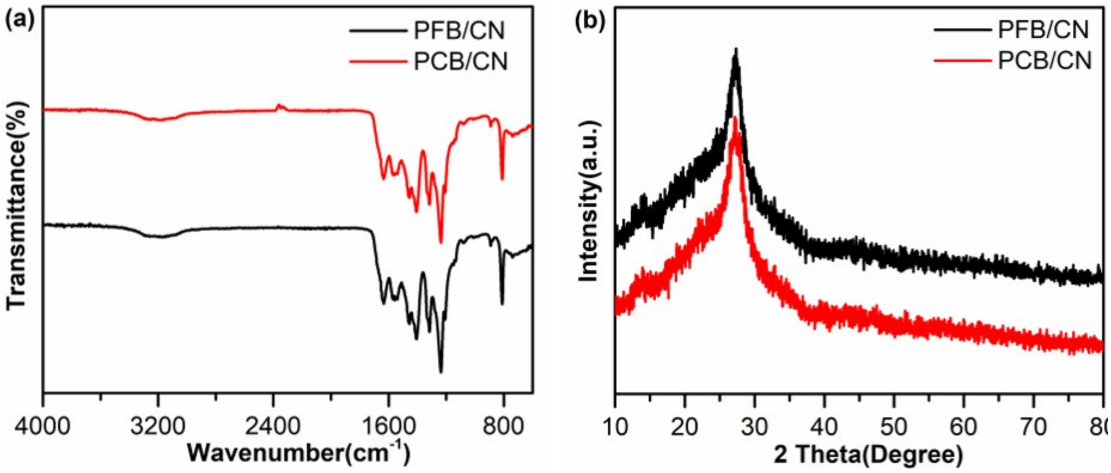

Fig.S7. (a) FTIR spectra; (b) XRD of **PFB**/CN and **PCB**/CN after photocatalytic reaction.

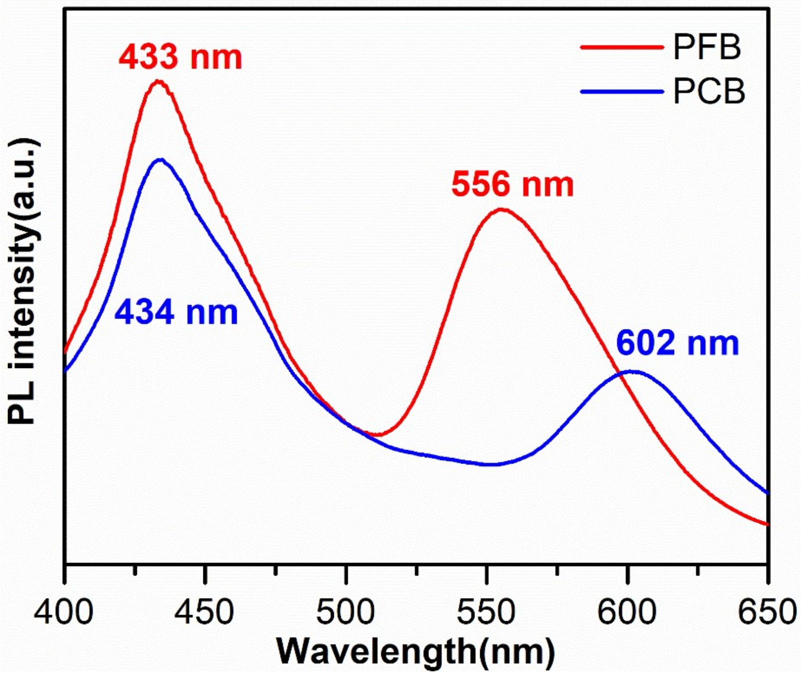

Fig.S8. Photoluminescence spectra of D-A conjugated polymer of **PFB** and **PCB**.

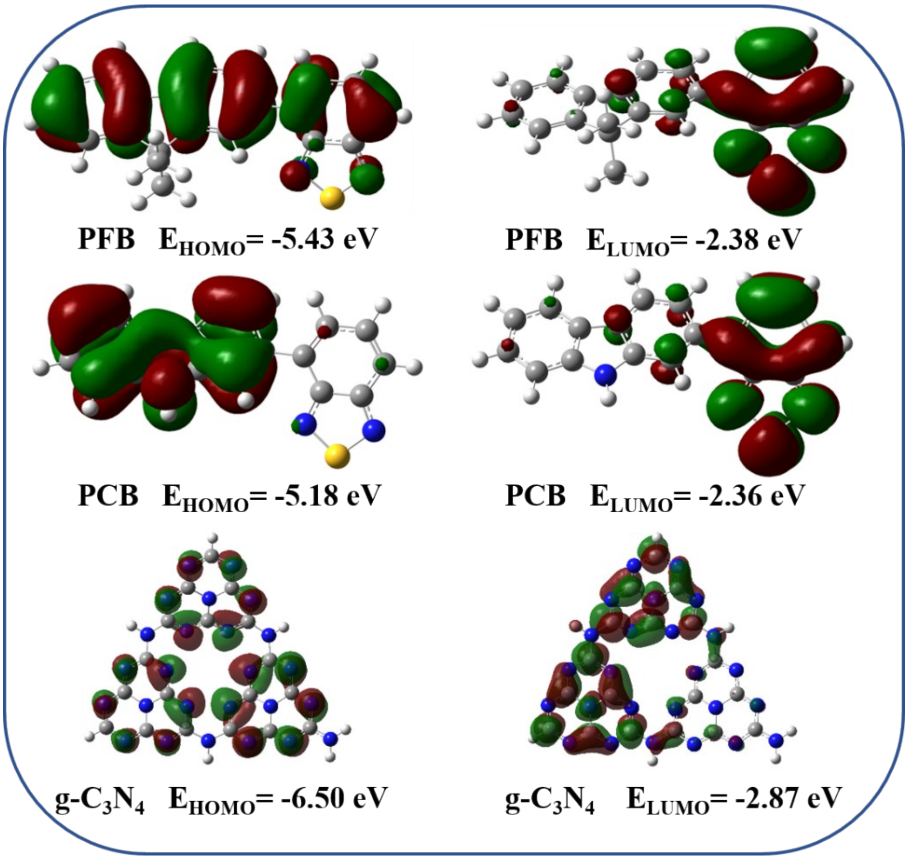

Fig.S9. B3LYP/6-31G* wave functions of the frontier molecular orbital in **PFB**, **PCB** and g-C_3N_4 with a chain length of n = 1. The grey ball: carbon atom; blue ball: nitrogen atom; yellow ball: sulfur atom; white ball: hydrogen atom.

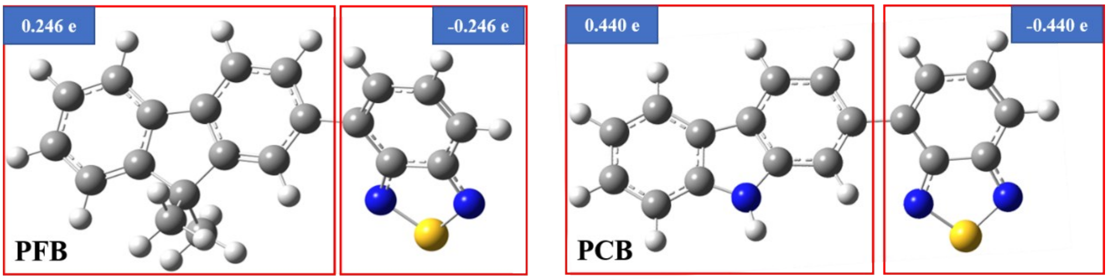

Fig.S10. The Mulliken charge analysis for **PFB** and **PCB**.

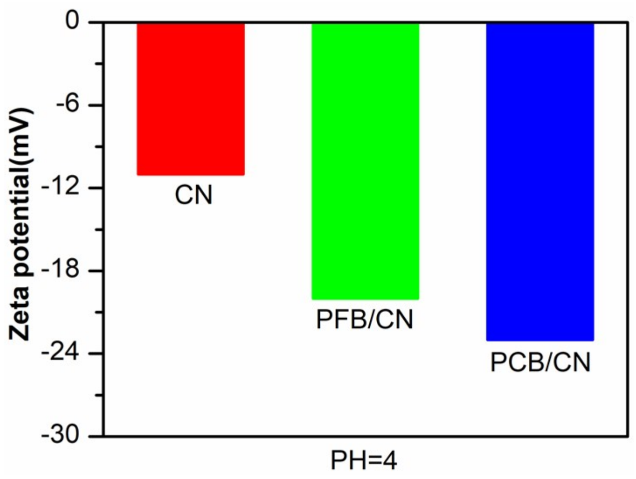

Fig.S11. Zeta potential tests pure CN and polymer/CN samples at pH = 4 in nitrogen atmosphere.

S8 Corresponding table in article

Table S1. Elemental composition (atom ratios) of samples according to XPS analysis

Sample	C/at %	N/at %	Oat %	S/at %	C/N
CN	41.1	53.1	5.8	0.0	0.77
PFB/CN	48.8	43.6	6.7	0.9	1.12
PCB/CN	44.7	48.1	6.4	0.8	0.93

Table S2. Relative ratios of two sulfur species determined by S 2p spectra for samples

	S2p3/2			S2p1/2		
Sample	Binding Energy(eV)	area	%	Binding Energy(eV)	area	%
CN	—	—	—	—	—	—

PFB/CN	166.4	794.4	54.4	165.4	665.5	45.6
PCB/CN	166.4	2071.0	73.3	165.4	753.6	26.7

Table S3. Relative ratios of two carbon species determined by C 1s spectra for samples

	C=C			N=C–N		
Sample	Binding Energy(eV)	area	%	Binding Energy(eV)	area	%
CN	284.6	5834.1	23.8	288.1	18622.5	76.2
PFB/CN	284.6	15388.4	37.2	288.18	26020.6	62.8
PCB/CN	284.6	19083.3	44.6	288.10	23687.6	55.4

Table S4. Relative ratios of four nitrogen species determined by N 1s spectra for samples

	C= N–C			$N–C_3$			π excitation		
Sample	Binding Energy(eV)	area	%	Binding Energy(eV)	area	%	Binding Energy(eV)	area	%
CN	398.92	30583.0	65.50	400.68	14257.0	30.60	404.7	1826	3.90
PFB/CN	398.88	40830.3	71.80	400.62	15357.9	27.00	404.58	678.6	1.20
PCB/CN	398.87	37680.6	71.00	400.60	14452.6	27.20	404.54	913.7	1.80

S9 References

1. F. Yu, Z. Wang, S. Zhang, H. Ye, K. Kong, X. Gong, J. Hua, H. Tian, Adv. Funct. Mater. 28 (2018) 1804512–1804524.
2. X. Chen, S. Shen, L. Guo, S. Mao, Chem. Rev. 110 (2010) 6503–6570.
3. W. Hehre, R. Ditchfield, J. Pople, J. Chem. Phys, 56 (1972) 2257–2261.